Measurement of *K*-shell photoelectric absorption parameters of Hf, Ta, Au, and Pb by an alternative method using a weak β-particle source

S. V. Nayak and N. M. Badiger*
Department of Physics, Karnatak University, Dharwad 580 003, India
(Received 5 October 2005; revised manuscript received 17 November 2005; published 6 March 2006)

Both the *K* absorption edge and the *K*-shell photoelectric cross section have been determined for Hf, Ta, Au, and Pb by using a continuous external bremsstrahlung (EB) radiation from a weak β source. In this method the EB photons produced in a nickel foil by the β particles from a weak ^{90}Sr-^{90}Y β source are incident on a target and the spectrum of the transmitted photons is recorded with a high-purity Ge detector coupled to an 8000 multichannel analyzer. The transmitted spectrum exhibits a sharp fall in intensity at the *K*-shell binding energy; and such a fall is used to determine both the *K*-absorption edge and the photoelectric cross section of the target.

DOI: 10.1103/PhysRevA.73.032707 PACS number(s): 32.80.Fb, 32.80.Cy, 32.30.Rj

I. INTRODUCTION

Interaction of γ radiation with matter has been a subject of experimental as well as theoretical interest again in recent years in view of its applications in several fields such as radiation physics, radiation biology, and industry [1–3]. It is well known that γ radiation interacts with matter mainly through photoelectric absorption, Compton scattering, and pair production processes. Low-energy γ photons ($E<100$ keV) interact with high-*Z* target atoms predominantly through the photoelectric effect resulting in emission of photoelectrons, x-ray photons, and Auger electrons from the target. The photoelectric effect involving the *K*-shell electron can take place only if the incident photon energy is greater than the binding energy of the *K*-shell electron. Theoretical values of atomic photoelectric cross sections for all the elements at various energies have been calculated by several researchers [4–6]. The experimental values of photoelectric cross sections for different elements at various energies have been measured by several investigators using different methods [7–13]. Normally two geometrical configurations are adopted for measuring the *K*-shell photoelectric cross section; the broad- [14] and the narrow-beam [7,15] geometrical configurations.

In the broad-beam geometrical configuration, the intensity of the *K* x-ray photons emitted from the target atoms is measured when the *K*-shell vacancies are produced in the target atoms by an incident beam of monoenergetic γ photons. The photoelectric cross section is determined by knowing the experimental *K*-shell fluorescence cross section, theoretical values of fluorescence yield, and jump ratio. Fields such as radiation biology, food and agriculture, and medicine demand the broad-beam geometrical configuration [16].

In the narrow-beam geometrical configuration, the intensity of incident photons that are transmitted through the target is measured. Collimators are used to prevent the photons scattered by the target atoms from entering into the detector. The attenuation cross section for the target atom for discrete monoenergetic γ rays (from radioactive sources) at energies below and above the *K* edge is measured. A plot of attenuation cross section for these discrete photon energies reveals a sudden drop at the *K* absorption edge. The cross section at the lower-energy edge is the sum of cross sections due to coherent scattering, Compton scattering, and the *L* and *M* photoelectric effect only. On the other hand the cross section at the upper-energy edge involves not only the above processes but also the *K*-shell photoelectric effect. Therefore the difference between the upper edge and lower edge at the *K* absorption edge gives the *K*-shell photoelectric cross section. Several investigators have measured the photoelectric cross section at energies below and above the *K* absorption edge of the targets of many elements [15,19,20]. It is interesting to note that in this method, the total cross sections in the upper and lower branches are extrapolated to meet at the *K* absorption edge; the *K*-edge value is not measured in this method but is invariably taken from the table [18]. Therefore this method of determining the photoelectric cross section at the *K* edge involves the selection of a *K*-edge value either theoretically or experimentally.

However, when synchrotron radiation is used the energy of the incident radiation can be varied continuously and the *K*-edge and photoelectric cross section can be determined. So far measurements have been carried out for low- and medium-*Z* elements because the intensity of radiation from older synchrotrons decreases rapidly above 50 keV. But with modern synchrotrons such as ESRF, APS, and Spring-8, the measurement can be extended to high-*Z* elements also.

In the present work, we have shown that by using a weak β source both the *K*-shell photoelectric cross section and *K* absorption edge can be determined experimentally. We report our results for Hf, Ta, Au, and Pb elemental targets.

II. EXPERIMENTAL DETAILS

The experimental arrangement used in the present investigation is shown in Fig. 1. It consists of a weak ($\sim$10 μCi) ^{90}Sr-^{90}Y β source *S*, a nickel converter *C* (47.2 mg/cm^2), a perspex absorber *P* of thickness 10 mm, and a detector *D*. The β particles from source *S* produce external bremsstrahlung (EB) photons in the nickel converter

*Corresponding author. Fax: +91 836 274 7884. Email address: nagappa123@yahoo.co.in

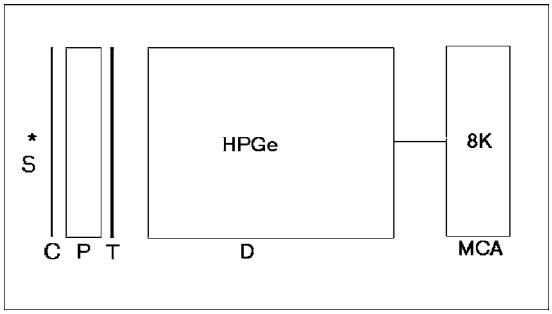

FIG. 1. Experimental arrangement for determining K-shell photoelectric absorption parameters. S, β source; C, nickel converter; P, perspex absorber; T, target foil; D, detector.

C. The high-energy β particles transmitted through the converter subsequently produce unwanted EB photons in the detector; to prevent these β particles from reaching the detector, the perspex absorber (P) is placed between the converter C and the detector D. The EB photons that pass through the target T are recorded by the detector D. The half-life of ^{90}Sr is 28.4 yr and ^{90}Y is in secular equilibrium with it. Because of the long half-life of ^{90}Sr, the intensity of β particles remains constant throughout the experiment. Each measurement of incident and transmitted spectra is carried out over a period of less than 20 h. So the EB photon intensity is absolutely constant.

Pure elemental targets of Hf, Ta, Au, and Pb are used in the present investigations. These targets were obtained from the Advent Research Material, England and were rolled to make thin and uniform foils. The spectrum of EB photons transmitted through a target is measured with an ORTEC high-purity Ge (HPGe) detector of the type GMX 10P. The detector has diameter of 49.6 mm, length of 47.1 mm, and a beryllium window of thickness 0.5 mm. The output of the detector is coupled to an 8000 multichannel analyzer, having ORTEC MAESTRO software. The detector is calibrated in the energy range from 10 to 100 keV using monoenergetic γ sources [21] of ^{57}Co (14.411, 122.061, and 136.473 keV), ^{241}Am (59.536 keV), and ^{109}Cd (88.034 keV). Calibration was done every time before and after a set of data was collected for each target. The least-square fit calibration constant is found to remain constant at 19.960 ± 0.001 eV per channel.

First the incident EB spectrum is recorded with the nickel converter C and the perspex absorber P in position. The measured EB spectrum transmitted through P is shown in Fig. 2(a). Next, the target T is placed in position and the spectrum of photons transmitted through T is recorded. A typical spectrum of the EB transmitted through a target is shown in Fig. 2(b) for Hf. From Fig. 2(b), we notice that the intensity of the transmitted EB photons suddenly decreases over an energy range of 1 keV between the photon energies of 64.87 and 65.89 keV; this is evidently due to the onset of the K-shell photoelectric effect. We also notice, below the steep fall, some x-ray peaks such as $K\alpha 1$, $K\alpha 2$, $K\beta 1$, and $K\beta 2$ of the target element. These peaks are due to the K-shell vacancies created by the EB photons in the target atoms. We notice in the figure that $K\beta 2$ and the steep fall at the K edge are not separated because of the low energy resolution of the detector (700 eV at 88 keV).

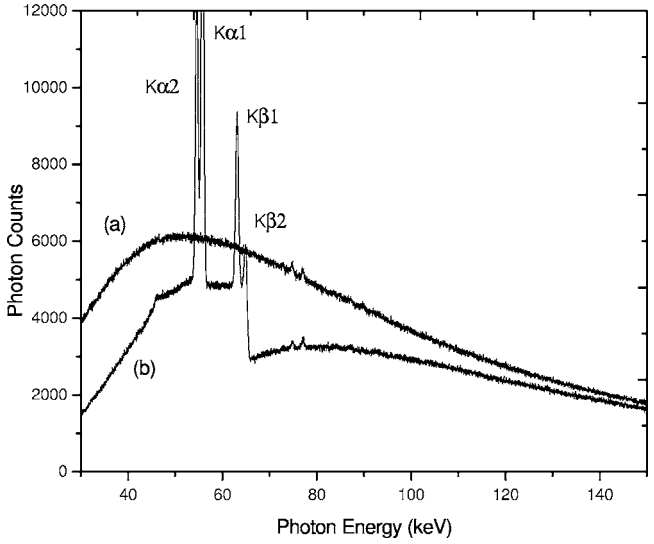

FIG. 2. Incident EB spectrum (a) and spectrum of EB photons in the presence of hafnium target (b) Scale: 1 channel=19.960 eV.

III. ANALYSIS OF DATA

A. Determination of photoelectric cross section

If I_0^i is the intensity of incident photons (in the absence of the target) and I_t^i is the intensity of the transmitted photons (in the presence of the target) at the EB photon energy E_i, we have

$$I_t^i = I_0^i e^{-(N_0 t/A)\sigma_e^i}$$

where A is the atomic mass of the target element, N_0 the Avogadro number, and t the thickness of the target foil in g/cm^2. The total cross section σ_e^i at E_i is given by

$$\sigma_e^i = \frac{A}{N_0 t} \ln\left(\frac{I_0^i}{I_t^i}\right). \quad (1)$$

Using experimentally measured I_t^i and I_0^i we have calculated σ_e^i for various E_i values.

In Fig. 3 we have plotted the experimentally determined σ_e^i values as a function of E_i over the energy range from 63.95 to 66.67 keV. We notice that the experimental values remain almost constant in the range from 63.95 to 64.51 keV, increase rapidly from 65.07 to 65.87, and again remain constant from 65.87 to 66.67 keV. We have omitted the counts due to the $K\beta 2$ x-ray peak. The sudden increase is attributed to the onset of the K-shell photoelectric effect. Because of the limited resolution of the detector the increase in K-shell photoelectric cross section takes place over a range of about 800 eV. In order to find accurately the total cross section σ_b below the K edge, the exact value of the K absorption edge E_k, and the total cross section σ_a above the K edge we have least-square fitted the sigmoidal function

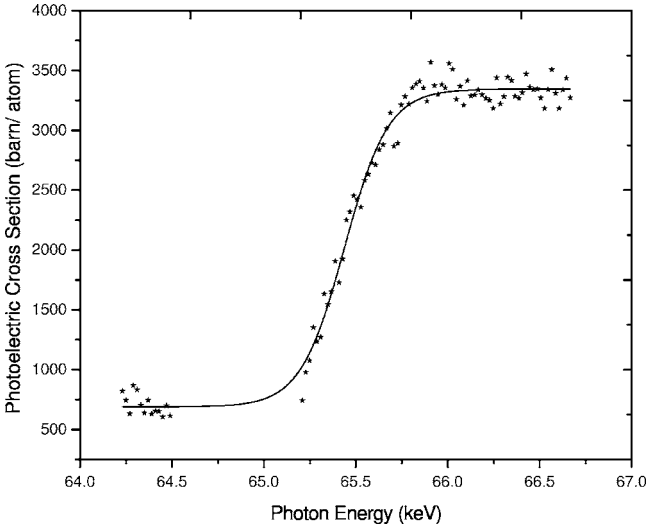

FIG. 3. The total *K*-shell photoelectric cross section of Hf target as a function of photon energy; ★ experimentally determined values; and—least-square fit sigmoidal function.

$$\sigma_e(E) = \frac{\sigma_b - \sigma_a}{1 + \exp\left(\frac{E - E_k}{dE}\right)} + \sigma_a \qquad (2)$$

to our experimental data. Here $\sigma_e(E)$ is the experimental value of the total cross section at photon energy E. The least-square fit sigmoidal function is shown as a smooth curve in Fig. 3. Needless to repeat that in the least-square fit we have omitted the counts in the energy range corresponding to the $K\beta 2$ x-ray peak. We see that there is excellent agreement between experimental points and the least-square fit curve.

The fact that the experimental points over the lower-energy part remain almost constant shows that all the processes which contribute to σ_b remain almost independent of energy over this energy range; similarly the fact that the experimental points remain almost constant over the higher-energy range again shows that all processes which contribute to σ_a remain almost independent of energy over this energy range. So the difference between these two constant values evidently is the *K*-shell photoelectric cross section at the *K* edge. The difference between the least-square fit values of σ_a and σ_b of the sigmoidal function is identified as the experimentally measured *K*-shell photoelectric cross section τ_k.

In this connection we may mention the following points relevant to dependability of our experimental measurement.

1. Uniformity of the target thickness

The uniformity of the target was checked by measuring the transmission of monochromatic γ rays over a small area of 1 mm diameter at four different locations of the target of 4 cm diameter. The targets were uniform within 1%. However, it may be pointed out that in this experiment the non-uniformity of the target does not play a critical role in yielding the photoelectric parameters.

TABLE I. The total photoelectric cross section for Hf and Pb targets (b/atom).

Trial	τ_k(Hf)	τ_k(Pb)
1	2621	1823
2	2662	1822
3	2688	1881
4	2597	1809
5	2654	1846
Mean	2644±45	1836±36

2. Efficiency of the detector

We may mention that the steep fall in the region of interest is only over the energy range of 2 keV. Evidently the variation of the efficiency of the detector over this narrow range of 2 keV is not significant enough to affect our measured values.

3. Reproducibility of the data

To ascertain the reproducibility of the data we have collected the data for each target thickness (of each element) five times each of the duration of 8 h to reduce statistical error in the counts. The five τ_k values obtained by sigmoidal fit agree with one another within 2%. Five trial values of τ_k for Hf and Pb targets are given in Table I. The mean values are taken as experimental values.

4. Effect of target thickness

In order to find the effect of target thickness on the measured τ_k values we repeated the experiment for two lead targets of thickness 54.37 and 110.1 mg/cm^2. The τ_k value for the 54.37 mg/cm^2 target was 1880 b/atom and that for the 110.1 mg/cm^2 target 1881 b/atom. The agreement is within 1%, showing that the method is independent of target thickness. The data were collected five times for the 110.1 mg/cm^2 target thickness. The mean value of the least-square fit is presented in Table I.

5. Effect of presence of other elements

Apart from the target, there are other elements present in the experimental arrangement such as the beryllium window of the detector, the perspex absorber, and oxygen and nitrogen in the environment. But they are all low-*Z* elements. The *K*-edge energies of these elements are far below those of the targets used. So their presence does not affect the spectrum in the region of our interest.

The final mean experimental values of τ_k for Hf, Ta, Au, and Pb are given in Table II.

B. Determination of *K* edge

Using a least-square fit sigmoidal function we have also determined the *K* absorption edge of the target atom. The first derivative of the sigmoidal function gives a Gaussian

TABLE II. K absorption edge and photoelectric cross section of elemental targets obtained using sigmoidal function. (t in mg/cm^2, E_k in keV, and τ_k in b/atom.)

Element	Z	t	E_k (expt.)	E_k (theory)	τ_k (expt.)	τ_k (theory)	% deviation
Hf	72	67.14	65.444	65.351 [5]	2644	2851 [5]	−7.2
				65.350 [17]		3130 [17]	−15.5
				65.350 [18]			
				65.438 [4]		2767 [4]	−4.4
				65.313 [22]			
Ta	73	69.76	67.514	67.416 [5]	2612	2749 [5]	−5
				67.420 [17]		2894 [17]	−9.7
				67.416 [18]			
				67.521 [4]		2666 [4]	−2
				67.400 [22]			
Au	79	46.76	80.78	80.725 [5]	1830	2213 [5]	−17
				80.720 [17]		2267 [17]	−19
				80.724 [18]			
				80.923 [4]		2142 [4]	−14.5
				80.713 [22]			
Pb	82	110.1	88.075	88.004 [5]	1836	1986 [5]	−7.6
				88.000 [17]		2013 [17]	−8.8
				88.004 [18]			
				88.263 [4]		1920 [4]	−4
				88.001 [22]			

distribution, as shown in Fig. 4 for Hf. The peak point of the distribution corresponds to the point of inflection E_k in the steep fall. We have identified the energy corresponding to the peak point as the K absorption edge of the target atom. We find that the five experimentally determined values of E_k of each element agree with one another within 1.2%; the mean value is taken as the final experimental E_k value. These values are given in Table II.

We may point out that the two mean E_k values obtained for the targets of thickness 54.37 and 110.1 mg/cm^2 of lead are found to be 88.085±0.01 and 88.075±0.01 keV, showing that the final value of E_k is also independent of the thickness of the target.

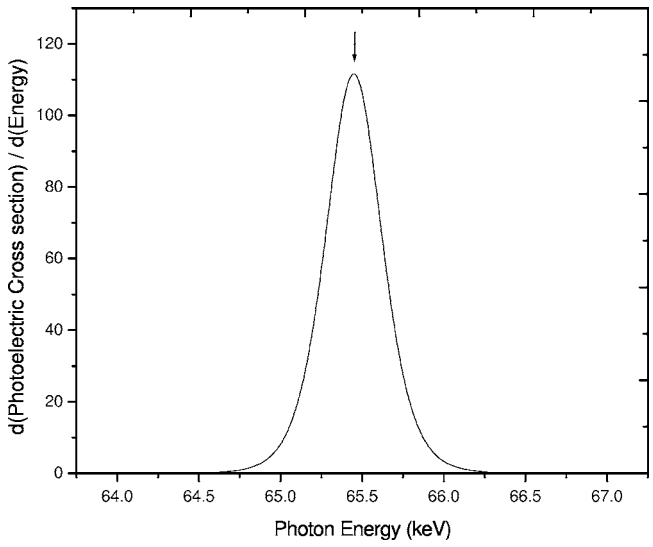

FIG. 4. The first-order derivative of the least-square fit sigmoidal function for hafnium.

IV. RESULTS AND DISCUSSION

Using this method we have determined the values of the τ_k and E_k for Ta, Au, and Pb. The least-square fit values are given in Table II. We have also presented the comparison of our experimental values of τ_k with the values predicted by various researchers in the same table. We notice from the table that the τ_k value of Hf agrees with the values predicted by Hubbell and Scofield within an error of 7% and differs from the value predicted by Veigele by 15%. The τ_k value of Ta agrees with that of Hubbell and Scofield within an error of 5% and differs from that of Veigele by 10%. The τ_k value of Au differs from the values predicted by Hubbell and Scofield and Veigele by about 15–19 %. However, the τ_k value of Pb agrees with the values predicted by Hubbell and Scofield and Veigele within an error of 9%.

Thus it is interesting to note that even though the energy resolution of the detector for monoenergetic γ photons at 88 keV is only about 700 eV, because of the use of the continuous bremsstrahlung spectrum and the possibility of fitting

the experimental data to a sigmoidal function whose derivative is a Gaussian distribution, it is possible to determine the *K*-shell binding energy of an atom with an accuracy of ±10 eV. Regarding achieving this accuracy we may mention the following points. A monochromatic x ray can also lead to a Gaussian distribution and a peak position of the Gaussian distribution can be determined with far greater accuracy than the resolution full width at half maximum of the detector. For instance we have fitted a Gaussian distribution to the $K\alpha$ peak of the Pb and Hf targets and found the peak positions to be 74.929±0.001 and 55.767±0.001 keV, respectively.

We also notice from Table II that our measured *K*-edge values slightly differ from the values given by some researchers. They have used a wavelength-dispersive spectrometer and their quoted values differ by several times the quoted errors. In our case we have used a HPGe detector which is of energy-dispersive type with lower energy resolution.

V. CONCLUSION

We have determined the *K*-shell photoelectric cross section and *K* absorption edge for Hf, Ta, Au, and Pb elemental targets using an alternative method. This method requires a weak β source and a single thin target of each element; the method can be extended to low-*Z* elements also. The most important point is that these measurements can be undertaken even by researchers who have no access to synchrotron radiation.

ACKNOWLEDGMENTS

One of the authors (S.V.N.) would like to thank the University Grant Commission, India, for financial support under the Faculty Improvement Programme (FIP) of the Xth five-year plan.

[1] J. H. Hubbell, Phys. Med. Biol. **44**, R1 (1999).
[2] J. H. Hubbell, X-Ray Spectrom. **28**, 215 (1999).
[3] L. Gerward, Radiat. Phys. Chem. **41**, 783 (1993).
[4] J. H. Scofield, LLNL Report No. UCRL-51326, 1973 (upublished).
[5] J. H. Hubbell and S. M. Seltzer, NISTIR Report No. 5632, 1995 (upublished).
[6] E. Storm and H. I. Israel, Nucl. Data, Sect. A **7**, 565 (1970).
[7] V. R. K. Murthy and K. R. S. Devan, Radiat. Phys. Chem. **71**, 671 (2004).
[8] A. Karabulut, A. Gurol, G. Budak, and M. Ertugrul, Nucl. Instrum. Methods Phys. Res. B **227**, 485 (2005).
[9] R. Nathuram, I. S. S. Rao, and M. K. Mehta, Phys. Rev. A **37**, 4978 (1988).
[10] S. K. Arora, K. L. Allawadhi, and B. S. Sarode, Phys. Rev. A **23**, 1147 (1981).
[11] C. T. Chantler, C. Q. Tran, Z Barnea, D. Paterson, D. Cookson, and D. X. Balaic, Phys. Rev. A **64**, 062506 (2001).
[12] R. Preseren and A. Kodre, Radiat. Phys. Chem. **55**, 363 (1999).
[13] T. K. Umesh and C. Ranganathaiah, Nucl. Instrum. Methods Phys. Res. B **5**, 472 (1984).
[14] H. A. Jahagirdar, B. Hanumaiah, and S. R. Thontadarya, Appl. Radiat. Isot. **44**, 875 (1993).
[15] M. L. Mallikarjuna, S. B. Appaji Gowda, K. E. Ganesh, R. Gowda, and T. K. Umesh, Nucl. Instrum. Methods Phys. Res. B **215**, 4 (2004).
[16] J. H. Hubbell, J. Res. Natl. Inst. Stand. Technol. **95**, 689 (1990).
[17] Wm. J. Veigele, At. Data **5**, 51 (1973).
[18] J. A. Bearden and A. F. Burr, Rev. Mod. Phys. **39**, 125 (1967).
[19] M. Tamura, T. Akimoto, Y. Aoki, J. Ikeda, K. Sato, F. Fujita, A. Homma, T. Sawamura, and M. Narita, Nucl. Instrum. Methods Phys. Res. A **484**, 642 (2002).
[20] M. Kefi, J-M. Andre, Y. Heno, G. Giorgi, and C. Bonnelle, Phys. Rev. A **45**, 2859 (1992).
[21] E. Browne and R. B. Firestone, *Table of Radioactive Isotopes* (Wiley-Interscience, New York, 1986).
[22] N. A. Dyson, *X-Rays in Atomic and Nuclear Physics* (Cambridge University Press, Cambridge, U.K., 1990).